An improved nearest neighbor method for the estimation of the gamma photon entry point in monolithic scintillator detectors for PET

Beekman, Freek J.; Schaart, Dennis R.; Van Dam, Herman T.; Seifert, Stefan; Vinke, Ruud; Dendooven, Peter; Löhner, Herbert

Published in:
IEEE Nuclear Science Symposuim and Medical Imaging Conference, NSS/MIC 2010

DOI:
10.1109/NSSMIC.2010.5874368

An Improved Nearest Neighbor Method for the Estimation of the Gamma Photon Entry Point in Monolithic Scintillator Detectors for PET

Herman T. van Dam, Stefan Seifert, *Member, IEEE*, Ruud Vinke, *Member, IEEE*,
Peter Dendooven, *Member, IEEE*, Herbert Löhner, *Member, IEEE*,
Freek J. Beekman, *Member, IEEE*, and Dennis R. Schaart, *Member, IEEE*

***Abstract*—Several improvements of the *k*-nearest neighbor (*k*-NN) method for the determination of the entry point (*x*,*y*) of a gamma photon in a monolithic scintillator PET detector have been investigated with the aim to obtain better spatial resolution and/or to enable faster detector calibration by reducing the amount of required reference data and by allowing for calibrating with a line source. These methods were tested on a dataset measured with a SiPM-array-based monolithic LYSO detector. It appears that ~10% to ~25% better spatial resolution can be obtained compared to the standard approach. Moreover, some of the improved methods using two orders of magnitude less reference data, yield essentially the same spatial resolution as the standard method, which reduces the time needed for calibration as well as entry point computation. Finally, line source calibration is shown to be possible with some of the methods, yielding better results than the standard method and allowing much faster and easier collection of the reference data.**

I. Introduction

THE *k*-nearest neighbor (*k*-NN) method has been shown to provide good performance for the determination of the gamma photon entry point in monolithic scintillator detectors [1, 2], but the calibration of the detector requires the acquisition of a large set of reference data by irradiating the crystal with annihilation quanta at a large number of known entry points and potentially at many different angles of incidence. Additionally, entry point estimation with the standard *k*-NN method involves an extensive calculation since the unclassified event is compared to a large number of reference events.

Yet, considering developments in faster and better FPGAs, high-bandwidth data transfer technologies, larger memories, and multi-core processing units, the high spatial resolution achievable with the nearest neighbor approach may still come within reach especially if the algorithms can be made more efficient.

Manuscript received November 12, 2010. (This work was supported by SenterNovem grant No. IS055019.

H. T. van Dam, S. Seifert, F. J. Beekman, and D. R. Schaart are with Delft University of Technology, Delft, 2629 JB, The Netherlands (corresponding author e-mail: d.r.schaart@tudelft.nl).

R. Vinke, P. Dendooven, and H. Löhner are with the KVI, University of Groningen, Groningen, 9747 AA, The Netherlands.

In the present work we investigate and compare several possible modifications of the standard *k*-NN method, as used for entry point estimation by Maas *et al*. [3], with the aim to either improve the spatial resolution when using a given amount of reference data, or, equivalently, to reduce the amount of reference data needed to achieve a given spatial resolution, allowing for faster calibration and position estimation. These improved methods make use of the fact that all NNs carry some information about the gamma entry point, which is utilized for example by smoothing or fitting the NN-histogram, or by means of the so-called categorical average patterns (CAP) method. Furthermore, several modified *k*-NN methods allowing for determining separately the reference data in the *x*- and *y*-directions are investigated. These methods are able to use reference data from a fast line source calibration, and, thus, require only $n_{pos,x} + n_{pos,y}$ calibration positions instead of $n_{pos,x} \times n_{pos,y}$ positions, where $n_{pos,x}$ and $n_{pos,y}$ denote the number of calibration positions in *x*- and *y*-directions, respectively. The different improved approaches, as well as combinations thereof, are tested on a dataset measured with a SiPM-based monolithic LYSO detector, by evaluating the spatial resolution of the modified estimation method as a function of the amount of reference data.

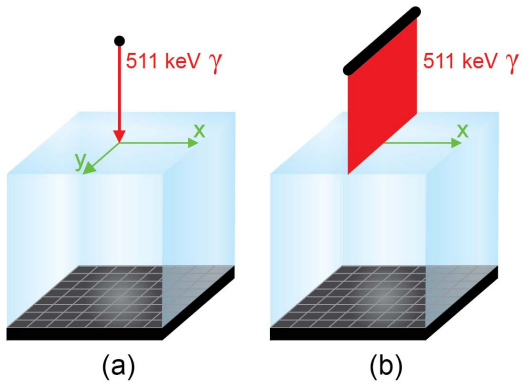

Fig. 1. (a) Illustration of a monolithic scintillator detector irradiated at a regular grid of *x*- and *y*-positions with a perpendicularly incident beam of gamma photons. (b) Detector irradiated along the y-axis at a certain x-position with a line source of gamma photons.

II. *K*-Nearest Neighbor Method (Standard Method)

The *k*-nearest neighbor (*k*-NN) method has been introduced by Fix and Hodges [4] and its application for the determination of the entry point of a gamma photon in a monolithic scintillator detector has been studied by Maas *et al*. [3]. In the latter work, a calibration measurement is performed in which a reference data set is collected by irradiating the monolithic scintillator detector with 511 keV photons at a grid of n_{pos} known positions (classes). Following the approach that the depth-of-interaction (DOI) may be obtained using some other method, the calibration needs only to be performed for perpendicularly incident photons (see Fig. 1a). For each irradiation position, the resulting light intensity distributions of n_{ref} reference events are recorded. All of these

$$n_{\mathrm{tot}} = n_{\mathrm{pos}} \cdot n_{\mathrm{ref}} \tag{1}$$

light patterns are normalized such that the sum of all detector signals equals unity. It should be noted that, due to differences in optical coupling, reflector, scintillator response, etc., each detector in principle requires its own reference data set.

The unknown entry point of an annihilation photon is subsequently estimated by calculating the Euclidean distances, i.e. the square root of the sum-of-squared-differences, of the measured light distribution to those of all events in the reference set. A subset of the reference data consisting of the *k* closest matches ('nearest neighbors') is selected and a histogram of their entry points is created. The entry point corresponding to the maximum value of the histogram, i.e. the most frequently occurring entry point, is assigned to the unclassified event. In case of multiple maxima, i.e. a tie, one of the maxima is selected randomly. It should be noted that a tie could also be solved by increasing or decreasing *k* until a single maximum is obtained [6].

The probability of misclassification for the standard *k*-NN method approaches the theoretical minimum, viz. the Bayes error probability, in the infinite sample case, i.e. if *k*, n_{pos}, and n_{ref} tend to infinity such that $k / n_{\mathrm{tot}} \to 0$ [7].

III. Improved Nearest Neighbor Algorithms

In practice, approaching the conditions for optimal performance of the *k*-NN method may be very time consuming. It requires the detector to be irradiated with a large number of annihilation quanta at many different known positions. Additionally, the resulting large reference dataset causes the entry point estimation to be computationally intensive. Moreover, the *k*-NN method is not guaranteed to be the optimal way of using the information contained in the neighborhood of unclassified patterns in the finite sample case [8].

Therefore, in this work alternatives to the standard *k*-NN method are investigated based on the fact that all nearest neighbors carry some information, which is more effectively used, e.g. by smoothing or fitting the NN-histogram, by combining reference data for each dimension analogous to calibrating with a line source, or by means of the categorical average patterns (CAP) method. These methods might be less sensitive to misclassification due to statistical fluctuations in case of small reference data sets and, therefore, yield equal results as for large reference data sets, allowing for faster calibration. All methods discussed below were tested using a cross-validation method described in section IV. It should be noted that many methods have been tested and that only the ones that appeared to perform best are discussed in this work.

A. Fit of the k-NN-Histogram (Fit Lorentzian)

In this method the *k* nearest neighbors of an unclassified light distribution are selected and a 2D-histogram of their entry points is created. So far this is similar to the standard *k*-NN method. Now, for cases that are not rare, we can assume that the irradiation coordinate closest to the true entry point has the highest probability of being present in the set of nearest neighbors and that this probability decreases for entry points further away from this point. Therefore, all points in the histogram carry information about the true entry point. Using more of this information, instead of only the most frequently occurring coordinate can reduce statistical fluctuations on the entry point estimation. Here, this is performed by fitting the histogram with a 2D Lorentzian shaped function using a log-likelihood method. Since the actual shape of the histogram is not *a-priori* known, several peak shaped functions were tested, of which the Lorentzian shaped function yielded the best results. The coordinate that corresponds to the peak position value of the fit is assigned to the unclassified event. It should be noted that this method allows for obtaining continuous coordinates.

B. Smoothed k-NN-Histogram (Smoothed)

The 2D entry point histogram of the set of *k* nearest neighbors is smoothed with a moving average filter of $n \times n$ bins. Here, $n = 5$ and, thus, each new bin value is based on the average of 25 bin values of the original histogram. Near the edges of the histogram the number of averaging bins is decreased at the side of the edge. The coordinate corresponding to the maximum value of the smoothed histogram is assigned to the unknown event.

C. Split 1D k-NN-Histograms (Split 1D Max)

In this method the *x*- and *y*-coordinate are obtained separately. First, only the *x*-coordinate of each reference event is used. The Euclidean distances of the unclassified light distribution to those of all reference events are calculated. Then, a 1D-histogram is created of the *x*-coordinates of the entry points of *k* nearest neighbors. The coordinate that corresponds to the maximum bin value is the estimated *x*-coordinate. A similar procedure is used to obtain the *y*-coordinate. This method is analogous to collecting reference data with a line source (see Fig. 1b). E.g., if the line source is oriented parallel to the *y*-direction and scanned along the *x*-direction, one obtains a reference dataset for the determination of the *x*-coordinate. The *y*-coordinate is then determined in an equivalent way.

D. Fit of the Split 1D k-NN-Histograms (Split 1D Fit)

This method is equal to the previous one, except that the coordinate assigned to the unknown event corresponds to the peak position of a Lorentzian fit of the 1D-histogram.

E. Categorical Average Patterns (CAP)

The classification scheme of the so-called categorical average patterns (CAP) method is somewhat different from the previous methods [9]. In this method the entry point is estimated by first calculating the Euclidean distances of the unclassified light distribution to those of all reference events at a single irradiation position. A subset of these reference events consisting of the k nearest neighbors is then selected and an average light distribution is calculated for this subset. This is repeated for each irradiation position in the reference dataset. Then, the Euclidean distances of the unclassified light distribution to all of the average light distributions are calculated. The coordinate corresponding to the minimum distance is assigned to the unclassified light distribution.

F. Categorical Average Patterns Smoothed (CAP Smoothed)

This method is equal to the previous one, except that the obtained set of distances of the unclassified light distribution to all of the average light distributions is smoothed with a moving average filter, similar to the filter described in section III.B.

G. Categorical Average Patterns 1D (CAP 1D Min)

In this method the x- and y-coordinate are obtained separately. First, only the x-coordinate of each reference event is used. The Euclidean distances of the unclassified light distribution to those of all irradiation positions with one specific x-coordinate are calculated. A subset of these reference events consisting of the k nearest neighbors is then selected and an average light distribution is calculated for this subset. This is repeated for all x-coordinates of the irradiation positions. Then, the distances of the unclassified light distribution to all average light distributions are calculated. The x-coordinate corresponding to the minimum distance is assigned to the unclassified light distribution. A similar procedure is used to obtain the y-coordinate. This method is analogous to collecting reference data with a line source, similarly to the 'split 1D' methods described in sections III-C and III-D.

IV. Experimental Methods

Measurements were performed on a monolithic scintillator detector based on a 4 × 4 pixel SiPM array optically coupled to a 13.2 mm × 13.2 mm × 10 mm LYSO crystal. Reference data were collected by irradiating the detector at a rectangular, equidistant grid of positions with a pitch of 0.25 mm and covering the entire front surface of the crystal using a perpendicular 511 keV gamma photon beam with a diameter of ~0.64 mm. A detailed description of the experiments can be found in [2].

A. Spatial Resolution

The spatial resolution was determined using a cross-validation method, i.e. the leave-one-out method described by Maas *et al.* [1]. The estimated coordinates are subtracted from the corresponding irradiation coordinates and a 2D-histogram is created, representing the detector spatial response. In this work the ~0.64 mm width of the test beam is much smaller than the detector spatial response and, therefore, the histogram approximates the point spread function (PSF) [10]. Since for small sample cases the PSF suffers from low statistics, the histogram was fitted with an inverse polynomial shaped function

$$f_{\mathrm{fit}} = \frac{p_1}{1 + p_4\left(p_2 x^2 + p_3 y^2\right) + p_5\left(p_2 x^2 + p_3 y^2\right)^2}, \tag{2}$$

where p_i are fitting parameters. This function has no physical meaning, but it was chosen from a set of tested fitting functions, because it appeared to fit the PSFs best. An average value of the full width at half maximum (FWHM) and the full width at tenth maximum (FWTM) was calculated of the cross sections of the fit in the x- and y-directions as well as the two directions with a 45 degrees angle to the x- and y-direction. This was repeated for different numbers of nearest neighbors and the minimum FWHM and corresponding FWTM were taken as measures of the spatial resolution.

Each entry point estimation method described in section III was tested for different numbers of reference events per irradiation position n_{ref} and for different total amounts of reference data n_{tot}. This was achieved by removing data from the full reference data set. In the case that n_{tot} was varied both n_{ref} and n_{pos} were decreased. If the number of events per irradiation position being removed from the full reference set was larger than n_{ref}, the discarded events were used to create an additional equivalent reference data set with an equal value of n_{ref}. In this way, a mean value and a standard deviation of the spatial resolution were obtained for part of the cases.

V. Results and Discussion

In this work the error bars indicate the standard deviation arising from the results of equivalent reference datasets as discussed in section IV-A.

A. Spatial Resolution

Fig. 2a and 2b show the spatial resolution in terms of FWHM and FWTM, respectively, calculated as an average over the entire detector surface as a function of the number of reference events per irradiation position n_{ref}, where the irradiation grid spacing was kept constant at 0.25 mm. It appears that all alternative methods yield a better spatial resolution, FWHM as well as FWTM, than the standard method. This improvement varies from ~10% to ~25% depending on n_{ref}.

More specifically, when comparing the CAP methods to their equivalent 'normal' methods, i.e. standard method vs.

CAP, smoothed vs. CAP smoothed, and split 1D max vs. CAP 1D min, the CAP versions perform better. This is attributed to the fact that the CAP entry point estimation methods intrinsically use more information contained in the reference events.

Furthermore, the CAP smooth method outperforms all other methods in terms of FWHM, whereas the two fitting methods give better results than the others in terms of FWTM. These two fitting methods yield an almost constant value for the spatial resolution as a function of n_{ref}, i.e. ~1.85 mm for FWHM and ~4.25 mm for FWTM.

The 1D methods perform at least as well and in most cases even better than the corresponding 2D method. This could be explained by the fact that, given a total number of reference events, there is more reference data per 1D coordinate. An important advantage of these 1D methods, being equivalent to irradiating with a line source instead of a beam, is that they would allow for much faster calibration.

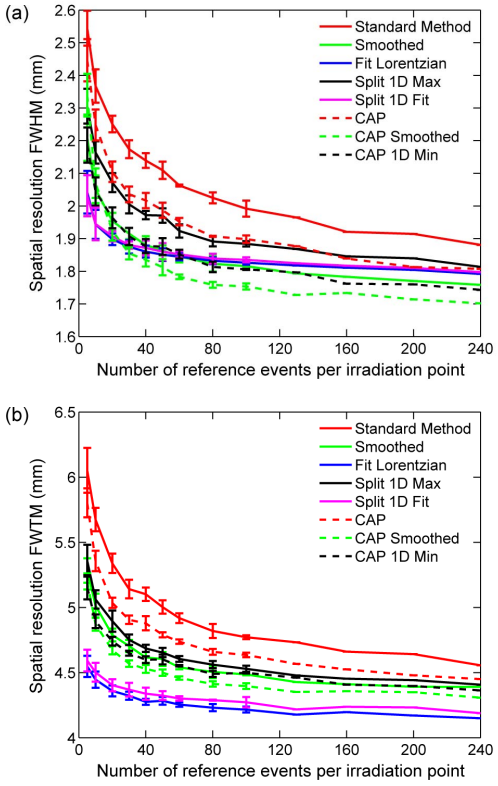

Fig. 2. Spatial resolution in terms of (a) FWHM and (b) FWTM calculated as an average over the entire detector surface as a function of n_{ref} for all methods analyzed using a constant irradiation grid spacing of 0.25 mm.

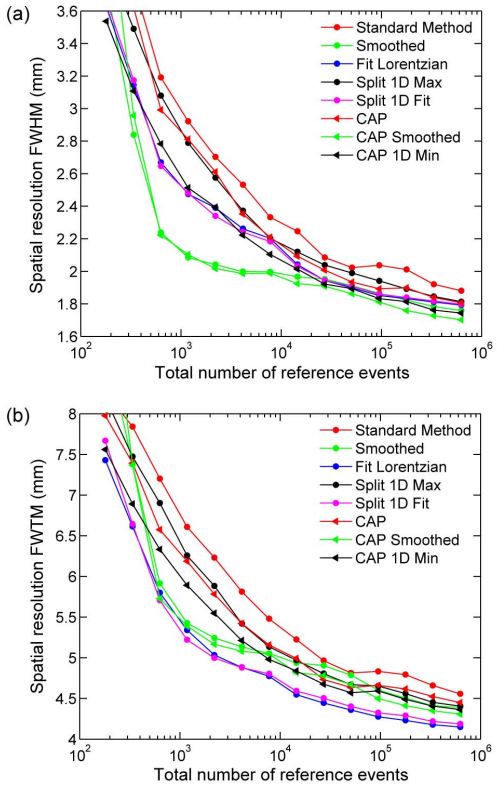

Fig. 3. Spatial resolution in terms of (a) FWHM and (b) FWTM calculated for the entire detector surface a function of n_{tot} for all methods analyzed where both the irradiation grid spacing and the number of reference events per irradiation point were varied.

Fig. 3a and 3b show the spatial resolution in terms of FWHM and FWTM, respectively, calculated as an average over the entire detector surface as a function of the total number of reference events n_{tot}. Each value of n_{tot} in general allows different combinations of n_{ref} and n_{pos} (see equation 1), each yielding different values for the spatial resolution. This should be taken into account, when reducing the amount of reference data to speed up calibration measurements. However, to provide a clear view of the spatial resolution in Fig. 3a and 3b, n_{tot} was binned with logarithmically increasing bin size and for each bin only the best spatial resolution is displayed as a function of the bin center.

Also in this case all alternative methods give a better spatial resolution than the standard method at almost all n_{tot}, in terms of FWHM as well as FWTM. Moreover, the CAP smooth method, the CAP 1D Min method, as well as the fitting methods, require ~10 to ~20 times less reference events than the standard method to obtain the same spatial resolution. Furthermore, the two smoothing methods yield a spatial resolution in terms of FWHM that is only slightly deteriorated at ~200 times less reference events, i.e. ~2.0 mm compared to ~1.9 mm. This means that with these methods the detector may be calibrated considerably faster.

VI. Conclusions

We have compared various methods for improving the standard *k*-nearest neighbor method used to determine the gamma photon entry point in monolithic scintillator detectors for PET. Better spatial resolution can be obtained by utilizing the information of the full set of nearest neighbors instead of only the one occurring most often. The CAP nearest neighbor methods were shown to perform better than their standard equivalent methods. Improvements in spatial resolution of ~10% to ~25% were achieved depending on the number of reference events.

Additionally, several presented alternative methods require ~10 to ~20 times less reference events than the standard method to obtain the same spatial resolution. The two smoothing methods yield a spatial resolution in terms of FWHM that is only slightly deteriorated at ~200 times less reference events, i.e. ~2.0 mm compared to ~1.9 mm. Using these methods the detector can be calibrated considerably faster.

Moreover, the methods equivalent to calibrating with a line source yielded considerably better results than the standard method while allowing for a much faster and easier collection of the reference data.

When a calibration measurement with a smaller total number of reference data is performed, it should be taken into account that there may be a combination of the number of reference events per irradiation position and the number of irradiation positions that provides an optimum spatial resolution.

A more detailed study of the improved *k*-NN methods including bias and spatial resolution as a function of the gamma photon entry point will be published in the near future.

References

[1] M. C. Maas, D. R. Schaart, D. J. van der Laan, P. Bruyndonckx, C. Lemaître, F. J. Beekman, et al., "Monolithic scintillator PET detectors with intrinsic depth-of-interaction correction," *Phys. Med. Biol.*, vol. 54, pp. 1893–1908, 2009.

[2] D. R. Schaart, H. T. van Dam, S. Seifert, R. Vinke, P. Dendooven, H. Löhner, *et al.*, "A novel, SiPM-array-based, monolithic scintillator detector for PET," *Phys. Med. Biol.*, vol. 54, pp. 3501–3512, 2009.

[3] M. C. Maas, D. J. van der Laan, D. R. Schaart, J. Huizenga, J. C. Brouwer, P. Bruyndonckx, S. Léonard, *et al.*, "Experimental characterization of monolithic-crystal small animal PET detectors read out by APD arrays," *IEEE Trans. Nucl. Sci.*, vol. 53, no. 3, pp. 1071–1077, Jun. 2006.

[4] E. Fix, J. L. Hodges, "Discriminatory analysis, nonparametric discrimination: Consistency properties," Technical Report4, USAF School of Aviation Medicine, Randolph Field, TX, 1951.

[5] T. Ling, T. K. Lewellen, and R. S. Miyaoka, "Depth of interaction decoding of a continuous crystal detector module," *Phys. Med. Biol.*, vol. 52, pp. 2213–2228, 2007.

[6] T. Bailey, and A. K. Jain, "A Note on Distance-Weighted *k*-Nearest Neighbor Rules," IEEE Trans. Syst., Man, Cybern., vol. 8, no. 4, pp. 311–313, Apr. 1978.

[7] T. M. Cover, and P.E. Hart, "Nearest Neighbor Pattern Classification," *IEEE Trans. Inf. Theory*, vol. 13, no. 1, pp. 21–27, 1967.

[8] T. Denoeux, "A *k*-Nearest-Neighbor Classification Rule Based on Dempster-Shafer Theory," *IEEE Trans. Syst., Man, Cybern.*, vol. 25, no. 5, pp. 804–813, May 1995.

[9] S. Hotta, S. Kiyasu, and S. Miyahara, "Pattern Recognition Using Average Patterns of Categorical *k*-Nearest Neighbors," *IEEE Proc. of the 17th International Conference on Pattern Recognition (ICPR'04)*, vol. 4, pp. 412–415, 2004.

[10] M. C. Maas, D. J. van der Laan, C. W. E. van Eijk, D. R. Schaart, F. J. Beekman, P. Bruyndonckx, *et al.*, "Model of the point spread function of monolithic scintillator PET detectors for perpendicular incidence," *Med. Phys.*, vol. 37, no. 4, pp. 1904–1913, Apr. 2010.